

## Fluorination Induced Etching Selectivity of Boron Nitride Phases

R. Q. Zhang,\* Dongju Zhang, Y. L. Zhao, and S. T. Lee

*Center of Super-Diamond and Advanced Films (COSDAF) & Department of Physics and Materials Sciences, City University of Hong Kong, Hong Kong S.A.R., China*

*Received: December 15, 2003; In Final Form: March 23, 2004*

Selective etching by hydrogen for different carbon phases is pivotal in enabling the synthesis of diamond using low-pressure chemical vapor deposition (CVD). However, this is not the case in the CVD synthesis of cubic boron nitride (c-BN). Here, by carrying out a systematic atomic-level study using the frontier orbital theory based on *ab initio* calculations, we show that, upon fluorination at the boron site, the etching selectivity of both hydrogen and fluorine for different boron nitride phases is significantly enhanced. By examining the electronic structural change, we found that the etching selectivity enhancement relates to the boundary saturation improvement upon fluorination. Moreover, fluorination also enhances the structural stability, particularly at the surface layers, providing a suitable environment for maintaining a proper charge transfer between boron and nitrogen atoms, which is the key factor for determining reactivity and stability. The enhanced etching selectivity would facilitate the CVD synthesis of high-quality cubic boron nitride films.

### Introduction

Since cubic boron nitride (c-BN) has many properties similar or superior to diamond, such as extreme hardness (which is second only to that of diamond), high thermal conductivity, good chemical inertness, and wide band gap capable of p- and n-type doping, great effort has been made to synthesize c-BN via various chemical vapor deposition (CVD) and physical vapor deposition (PVD) techniques. However, high-quality, single-phase c-BN films have been found to be extremely difficult to synthesize by CVD techniques due to the absence of selective etchants for the two BN phases (hexagonal and cubic). This is in contrast to the preferential etching of the  $sp^2$ -bonded graphitic phase over the  $sp^3$ -bonded diamond phase by hydrogen, which is a key factor in the successful CVD synthesis of high-purity diamond films.<sup>1,2</sup> Due to the failure of CVD, PVD has been the only technique to synthesize polycrystalline c-BN depositions. However, the high internal stress in PVD c-BN films has posed many problems, such as film delamination. New approaches—in particular, ones that adopt a mild CVD—to overcome the difficulties need exploring. Toward this aim, the details of the deposition processes and the reasons for the failure of such approaches need to be understood.

In previous works,<sup>3,4</sup> we elucidated the difficulty in obtaining c-BN of high phase purity via CVD with frontier orbital theory based on *ab initio* Hartree–Fock calculations. The study revealed a remarkable difference in the reactivity of hydrogen with  $sp^2$ - and  $sp^3$ -bonded carbon phases, which facilitates the phase selectivity in the CVD of diamond by adopting a high concentration of hydrogen, consistent with what was revealed in recent experiments. In contrast, the difference in the reactivity of the hydrogen species over h-BN and c-BN phases was found to be small, which explains the absence of etching selectivity of the hydrogen species over different BN phases. Prompted by this success in elucidating experimental observations, we use a similar approach to search for ways to stabilize the c-BN surface and suppress the formation of hexagonal boron nitride (h-BN).

Recently, experiments have shown that h-BN is etched preferentially in comparison to c-BN in fluorine-containing systems.<sup>5–9</sup> It has been found that h-BN was etched 6 times faster than c-BN by fluorine. Attempts were made to deposit BN films in B–N–F systems without applying a substrate bias.<sup>5,6</sup> Definitive evidence has been obtained confirming the formation of c-BN from a  $BF_3$ /Ar gas mixture.<sup>8</sup> To date, c-BN films containing crystallites as large as  $0.2\ \mu\text{m}$  can be synthesized by dc jet plasma CVD from an  $Ar-N_2-BF_3-H$  gas mixture.<sup>7,9</sup> A related theoretical study has indicated that fluorine is also effective in stabilizing the B(111) surface of c-BN.<sup>10</sup> To reach the goal of synthesizing high-quality c-BN films, the detailed roles of fluorine and hydrogen in the CVD synthesis of c-BN should be revealed, ideally at the atomic level. To this end, in this work, we examine the etching selectivity of hydrogen and fluorine over different BN phases with and without fluorination using the frontier orbital theory<sup>11,12</sup> based on Hartree–Fock (HF) molecular orbital calculations. The theoretical results are expected to provide useful guidance for improving the c-BN growth techniques.

### Models, Theory, and Computational Methods

Hexagonal and tetrahedral cluster models ( $B_xN_x$ ) ( $x = 3, 5, 7, 8, 9, 11, 12$ , and  $17$ ) were used to simulate the h-BN and c-BN phases, respectively. Dangling bonds exist at their boundaries not only for the h-BN clusters that require both B and N atoms being three-coordinated but also for the c-BN clusters that are composed of four-coordinated atoms of both B and N. The four coordination of B atom in the latter case is due to the material's significant ionic nature. Consequently, these dangling bonds must be terminated by suitable terminating species so as to simulate bulklike structural geometries even at the surfaces. Both H and F were used for the surface saturations, as they are the natural terminating species of BN phases during film deposition in H- and F-containing gas mixtures. Specifically, to model the fluorination of the h-BN and c-BN surfaces, fluorine atoms were used to saturate the surface dangling bonds

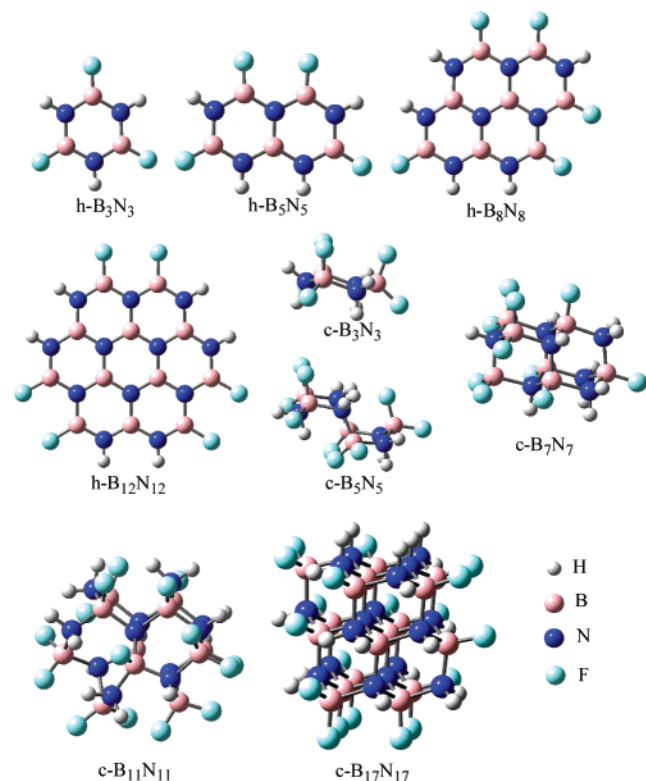


**Figure 1.** Hexagonal and tetrahedral clusters ( $B_xN_x$ ) ( $x = 3, 5, 7, 8, 9, 11, 12$ , and  $17$ ) used to simulate h-BN and c-BN phases.

of the boron atoms, while surface nitrogen atoms were saturated with hydrogen atoms for each cluster. Such clusters are henceforth referred to as F-terminated BN, denoted as  $B_xN_x(F)$ .

For the purposes of comparison, the corresponding BN clusters where all dangling bonds are saturated by hydrogen atoms were also used and are referred to as H-terminated BN clusters, denoted as  $B_xN_x(H)$ . Figure 1 shows the structures of the chosen  $B_xN_x(F)$  clusters.

The frontier orbital theory<sup>11,12</sup> states that the reactivity between two molecules is inversely proportional to the energy difference between the highest occupied molecular orbital (HOMO) (the lowest unoccupied molecular orbital (LUMO)) of one molecule and the LUMO (HOMO) of the other. The smaller the value of the HOMO–LUMO difference, the more reactive is the chemical reaction. Using these concepts of frontier orbital theory, we have previously obtained important information about reactivities between two interacting species<sup>13,14</sup> for a few widely concerned experiments. We again apply this approach in the present work to reveal the reactivities of the hydrogen and fluorine species on boron nitride clusters by comparing the HOMO–LUMO difference between them. The most reactive atoms of the interacting system were identified using a decomposition technique of density of states (DOS),<sup>15</sup> which is particularly convenient and efficient for a large system, as illustrated in a previous study that we conducted.<sup>16</sup> By using the technique, the total DOS of a system can be projected onto its constituent atoms to deduce how the individual atoms contribute to the total electronic structures. This would provide quantitative information about the detailed electronic properties, such as the difference in reactivity of constituent atoms.

To obtain a reliable result from the first principal calculation, it is essential to select a suitable level of theory that can handle a medium-sized system without loss of basic accuracy. As we proved in previous work,<sup>3,4</sup> the Hartree–Fock method is adequate for predicting the eigenvalues corresponding to the

**TABLE 1: Energies of HOMOs and LUMOs and Energy Gaps (in hartree) Determined with HF/6-31G\*\* and MP2/6-31G\*\* Approaches**

|      | HF/6-31G**     | MP2/6-31G** |
|------|----------------|-------------|
|      | h- $B_3N_3(H)$ |             |
| HOMO | −0.402 53      | −0.400 83   |
| LUMO | 0.177 81       | 0.176 68    |
| gap  | 0.580 34       | 0.577 51    |
|      | h- $B_3N_3(F)$ |             |
| HOMO | −0.427 29      | −0.428 97   |
| LUMO | 0.213 28       | 0.206 62    |
| gap  | 0.640 57       | 0.635 59    |
|      | c- $B_3N_3(H)$ |             |
| HOMO | −0.411 85      | −0.410 55   |
| LUMO | 0.186 29       | 0.182 80    |
| gap  | 0.598 14       | 0.593 35    |
|      | c- $B_3N_3(F)$ |             |
| HOMO | −0.525 49      | −0.529 12   |
| LUMO | 0.169 67       | 0.161 96    |
| gap  | 0.695 16       | 0.691 08    |

frontier molecular orbitals. In this work, we again adopt the Hartree–Fock method to optimize the geometries and subsequently obtain the electronic structures of the clusters. For polar compound systems, such as the present BN systems including both H- and F-terminated clusters, it is necessary to use a suitably flexible basis set in the calculation to give a reliable description of the valence shell orbitals of the atoms. Diffuse functions are usually considered important for negatively charged systems. However, they have been found to be incorrect for predicting the LUMO value due to the localization of the electron at diffuse atomic orbitals.<sup>4,14,17</sup> Thus, basis sets with diffuse functions were not adopted here. The split-valence basis set with polarization functions is expected to give a good description of the present fluorine-containing BN systems. In our previous studies of BN systems, the 6-31G\*\* basis set, which includes polarization functions for all the atoms involved in a system, was found to be reliable for predicting meaningful frontier orbitals.

To further examine the accuracy of our approach for the current B–N–F systems, we have optimized the geometric structures and calculated the electronic structures at both the HF/6-31G\*\* and MP2/6-31G\*\* levels of theory for the following small BN clusters terminated by both H and F: h- $B_3N_3(H)$ , h- $B_3N_3(F)$ , c- $B_3N_3(H)$ , and c- $B_3N_3(F)$ . Table 1 compares the energies of HOMOs and LUMOs as well as the energy gaps so determined. Clearly the HF method predicts results similar to those from the MP2 method. The obviously overestimated gap values are attributed to the effect of finite cluster size and the deficiency of the atomic orbital theory. Nevertheless, as the present work relies on the relative HOMO–LUMO differences rather than their absolute value, the approach is adequate for the present study for the B–N–F systems. Hence, all of the calculations described in the following were performed at the HF/6-31G\*\* level of theory and were carried out using the Gaussian 98 package.<sup>18</sup>

## Results and Discussion

As mentioned above, it is crucial to find a way of stabilizing the c-BN phase and suppressing the formation of h-BN. The conventional view is that such a goal can be reached by finding a selective etching agent for the h-BN phase. Recent experiments<sup>5,6</sup> have proven that h-BN can be etched preferentially in a fluorine-containing gas mixture.<sup>5–9</sup> What is the role of fluorine during the growth of c-BN films? Why can the participation of

**TABLE 2: Energies (in hartree) of HOMO and LUMO of H-Terminated and F-Terminated BN Clusters Calculated at HF/6-31G\*\* Level of Theory**

|                                   | $B_xN_x(H)^a$     |                   |                               | $B_xN_x(F)^a$     |                   |                               | $\Delta\Delta E$<br>(7) = (6) - (3) |
|-----------------------------------|-------------------|-------------------|-------------------------------|-------------------|-------------------|-------------------------------|-------------------------------------|
|                                   | $E_{HOMO}$<br>(1) | $E_{LUMO}$<br>(2) | $\Delta E$<br>(3) = (2) - (1) | $E_{HOMO}$<br>(4) | $E_{LUMO}$<br>(5) | $\Delta E$<br>(6) = (5) - (4) |                                     |
| c-B <sub>3</sub> N <sub>3</sub>   | -0.411 46         | 0.186 49          | 0.597 95                      | -0.526 06         | 0.170 59          | 0.696 65                      | 0.098 70                            |
| c-B <sub>5</sub> N <sub>5</sub>   | -0.402 00         | 0.178 14          | 0.580 14                      | -0.516 78         | 0.155 59          | 0.672 37                      | 0.092 23                            |
| c-B <sub>7</sub> N <sub>7</sub>   | -0.354 63         | 0.139 86          | 0.494 46                      | -0.481 91         | 0.113 93          | 0.595 84                      | 0.101 38                            |
| c-B <sub>11</sub> N <sub>11</sub> | -0.349 58         | 0.158 20          | 0.507 78                      | -0.484 84         | 0.131 43          | 0.616 27                      | 0.108 49                            |
| c-B <sub>17</sub> N <sub>17</sub> | -0.326 20         | 0.115 42          | 0.441 62                      | -0.456 89         | 0.091 73          | 0.548 62                      | 0.107 00                            |
| h-B <sub>3</sub> N <sub>3</sub>   | -0.402 58         | 0.177 30          | 0.579 88                      | -0.427 78         | 0.213 21          | 0.640 99                      | 0.061 11                            |
| h-B <sub>5</sub> N <sub>5</sub>   | -0.380 20         | 0.160 67          | 0.540 87                      | -0.404 41         | 0.189 68          | 0.594 09                      | 0.053 22                            |
| h-B <sub>7</sub> N <sub>7</sub>   | -0.369 16         | 0.158 19          | 0.527 35                      | -0.393 41         | 0.180 59          | 0.574 00                      | 0.046 65                            |
| h-B <sub>12</sub> N <sub>12</sub> | -0.367 14         | 0.163 86          | 0.531 00                      | -0.390 92         | 0.174 64          | 0.565 56                      | 0.034 56                            |

<sup>a</sup>  $B_xN_x(H)$  and  $B_xN_x(F)$  denote the H-terminated and F-terminated BN clusters, respectively.

BF<sub>3</sub> improve the etching selectivity? To answer these questions, we study here the effects of hydrogen and fluorine etching over the H- and F-terminated BN phases since both H and F are involved in the above-mentioned experiments as important reactants. Although ionic forms of these species may be present in the CVD process, it has been argued that the related chemical reactivity (chemical bonding) is mainly determined by their neutrals,<sup>19</sup> considering the fact that the substrate in experiments is normally well grounded.

To determine the reason for the variance of etching selectivity before and after the fluorination of the BN phases, we first inspect the eigenvalues corresponding to the HOMO and LUMO ( $E_{HOMO}$  and  $E_{LUMO}$ ) for the atomic H and F, and the various H- and F-terminated BN clusters. Table 2 shows the calculated data for various clusters at the HF/6-31G\*\* level of theory. At the same level, the  $E_{HOMO}$  and  $E_{LUMO}$  of H atoms are calculated to be -0.498 23 and 0.095 02 hartree and those of F atoms -0.663 60 and 0.093 66 hartree, respectively. Obviously, the energy difference between the HOMO of BN clusters and the LUMO of H or F atoms is smaller than that between the LUMO of BN clusters and the HOMO of H or F atoms. According to the frontier orbital theory, the HOMO of the BN clusters and the LUMO of H or F atoms will determine the reactivities between them.

As revealed in our previous work,<sup>3,4</sup> the reactivities of atomic H with H-terminated h-BN and c-BN phases are so similar that a pure c-BN phase cannot be achieved via conventional CVD. Here, we have also analyzed the reactivity of fluorine atoms over two H-terminated BN phases. As shown in Table 2, for H-terminated BN clusters, the HOMOs of c-BN and h-BN are close, with the result that the reactivities of H or F with two BN phases are similar. Figure 2a shows the energy difference between the HOMO (LUMO) of the various BN clusters and the LUMO (HOMO) of H and F as a function of cluster size, where  $H(F)/c-B_xN_x(H)$  and  $H(F)/h-B_xN_x(H)$  denote the reactivities of H(F) over H-terminated cubic BN and hexagonal BN phases, respectively. Clearly, no obvious difference in the reactivities of H and F atoms over two BN phases is observed, indicating that neither H nor F selectively etches the hydrogen-terminated sp<sup>2</sup>-BN phase to facilitate the c-BN growth.

As observed in previous experiments,<sup>5,6</sup> h-BN is etched 6 times faster than c-BN by fluorine in BF<sub>3</sub>/Ar reactant gas. To rationalize the effective etching selectivity, we conjecture that the fluorination of BN phases resulting from attaching F to the boron atoms (or BF and BF<sub>3</sub> to the nitrogen atoms) of BN phases may play a crucial role. In addition, based on similar reactivities of atomic H and F over two BN phases, we suggest that H may also selectively etch h-BN under the fluorination of BN phases. To confirm these hypotheses, we inspect the reactivities of both

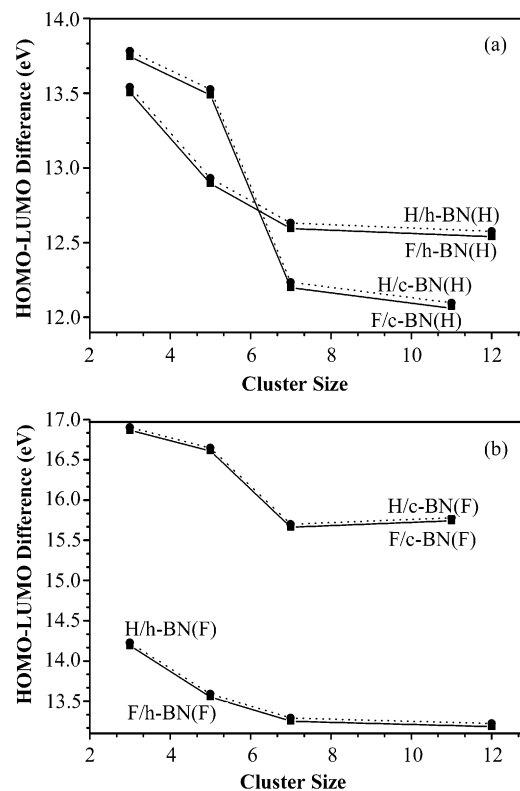


**Figure 2.** Energy difference between LUMOs of neutral hydrogen (dashed line) or fluorine (solid line) species and HOMOs of BN clusters of difference sizes for (a) H-terminated BN clusters,  $B_xN_x(H)$ , and (b) F-terminated BN clusters,  $B_xN_x(F)$ .

H and F atoms on the F-terminated BN phases. As shown in Table 2, when the B atoms of BN clusters are terminated by F atoms, the HOMOs of c-BN(F) are much lower than those of h-BN(F), with the result that the reactivity of h-BN(F) with the H and F etchants is much larger than that of c-BN(F). Figure 2b shows the reactivities of atomic H and F with two F-terminated BN phases, where  $H(F)/c-B_xN_x(F)$  and  $H(F)/h-B_xN_x(F)$  denote the reactivities of H(F) over F-terminated c-BN and h-BN phases, respectively. Obviously, the reactivities of both the H and F species are much larger during the F-terminated h-BN phase than those over the F-terminated c-BN phase. In other words, both the H and F species can selectively etch h-BN clusters due to their preference for the F-terminated h-BN phase over the F-terminated c-BN phase. This contrasts with the H-terminated BN phase, where neither the H nor the F species can selectively etch h-BN against c-BN. After the BN phases are fluorinated, the etching selectivities of the H and F species increase. This result is consistent with the experimental



observation that h-BN is etched 6 times faster than c-BN in the  $\text{BF}_3$ -containing system.<sup>5,6</sup>

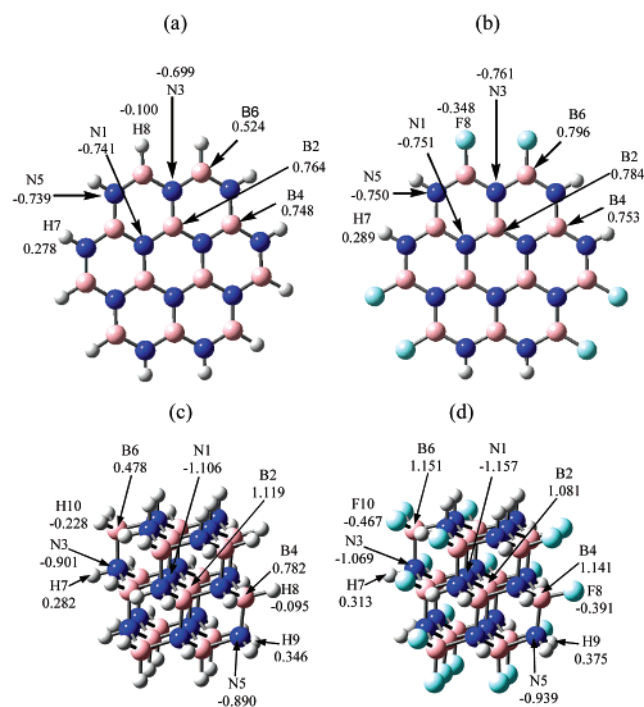
We note that all the curves in Figure 2 show an overall tendency to decrease as the cluster size increases, which is consistent with our previous reports for BN clusters<sup>3,4</sup> and for silicon and carbon clusters.<sup>19,20</sup> From the tendency shown in Figure 2, it is clear that the frontier orbital energy difference will level off when the cluster size is large enough for both the h-BN and c-BN phases, indicating that cluster size is also a factor in determining the reactivities of the H and F atoms over the BN phases. In the present study, we pay special attention to the relative etching effects of H and F over the BN phases with similar cluster sizes, as our main goal is to compare the relative etching selectivity of H and F over different BN phases.

Table 2 also presents the energy gap ( $\Delta E$ ) between the HOMO and LUMO and the variation of the energy gap ( $\Delta\Delta E$ ) before and after fluorination for various clusters. It can be seen that the gaps of c-BN clusters become larger, while the gaps of h-BN clusters are only slightly increased after fluorination. The values of  $\Delta\Delta E$  for the c-BN clusters are noticeably larger than those for the h-BN clusters, indicating a larger extent of modification of the electronic structure and thus the reactivity of the two BN phases by fluorination of the former than the latter.

While the gas-phase fluorine involved species stabilizes the tetrahedral BN configuration and etches the hexagonal BN back to the gas phase, the fluorination of c-BN and h-BN surfaces results in the formation of strong polar B–F bonds. Therefore, the CVD process for the growth of c-BN must be reinforced in order to reach equilibrium between stacking and etching at the BN surface. As indicated in recent experiments,<sup>5–9</sup> substrate bias must be used to activate such a stable c-BN surface bonded with fluorine.

To reveal the origin of etching selectivity enhancement, the charge distribution of the representative cubic ( $\text{c-B}_{17}\text{N}_{17}$ ) and hexagonal ( $\text{h-B}_{12}\text{N}_{12}$ ) boron nitride clusters before and after fluorination was examined. In a previous study we concluded that the charge distribution over a BN phase is crucial in determining its stability,<sup>21</sup> which closely relates to the electronic structure property and thus the reactivity. Our observation of the  $\beta$ -phase boron–carbon–nitrogen ( $\text{C}_2\text{BN}$ ) structure revealed that the segregation of  $\beta\text{-C}_{2n}(\text{BN})_n$  into the diamond and c-BN phases is a natural behavior due to the presence of C–BN junctions that prevent a sufficient charge transfer to satisfy the polar BN bond.<sup>21</sup> For the present systems, it is obvious that an improper charge distribution may occur at the surface due to the improper surface atom saturation when using hydrogen, and upon fluorination the boundary saturation would be considerably improved.

To reveal the details of charge distribution, the Mulliken charges of the representative atoms (distributed at the boundary and in the bulk) for four selected clusters are shown in Figure 3. The charges are marked close to the atoms or point to the corresponding atoms. The charge distributions of the boundary B and N atoms in the  $\text{h-B}_{12}\text{N}_{12}(\text{F})$  (Figure 3b) and  $\text{c-B}_{17}\text{N}_{17}(\text{F})$  (Figure 3d) clusters are obviously different from those in the  $\text{h-B}_{12}\text{N}_{12}(\text{H})$  (Figure 3a) and  $\text{c-B}_{17}\text{N}_{17}(\text{H})$  (Figure 3b) clusters. For the H-terminated clusters (Figure 3a,c), the hydrogen atoms that are improperly bonded with boron atoms carry negative charges due to the poor electronegativity of boron, leading to high instability of the local structure. Comparing the charge distributions between  $\text{h-B}_{12}\text{N}_{12}(\text{H})$  and  $\text{c-B}_{17}\text{N}_{17}(\text{H})$ , the former has a slightly higher negative charge at the H atoms associated with boron monohydride ( $-0.100$  to  $-0.095$  au), but a smaller



**Figure 3.** Mulliken charges for (a) H-terminated hexagonal boron nitride cluster  $\text{h-B}_{12}\text{N}_{12}(\text{H})$ , (b) F-terminated hexagonal boron nitride cluster  $\text{h-B}_{12}\text{N}_{12}(\text{F})$ , (c) H-terminated cubic boron nitride cluster  $\text{c-B}_{12}\text{N}_{12}(\text{H})$ , and (d) F-terminated cubic boron nitride cluster  $\text{c-B}_{12}\text{N}_{12}(\text{F})$ .

difference between the surface and bulk boron atoms ( $0.240$ – $0.337$  au for those associated with monohydride and  $0.641$  au for those associated with dihydride). Thus, the boundary saturation with hydrogen for the c-BN phase is far from satisfactory. It therefore causes increased reactivity to a larger extent than does the hexagonal phase, leading to a similarity in their reactivity, as we have revealed above. Upon fluorination, the improper charge distribution has been significantly improved. Due to the high electronegativity of fluorine, the electron density of the boundary B atoms in the c-BN clusters decreases as indicated by the corresponding net charge changes (from  $0.478$  au, as shown in Figure 3c, to  $1.151$  au, as shown in Figure 3d, for those atoms associated with dihydride; from  $0.782$  au, as shown in Figure 3c, to  $1.141$  au, as shown in Figure 3d, for those atoms associated with monohydride). Also, the electron density of the boundary N atoms increases (from  $-0.890$  au, as shown in Figure 3c, to  $-0.939$  au, as shown in Figure 3d, for those atoms associated with dihydride; from  $-0.901$  au, as shown in Figure 3c, to  $-1.069$  au, as shown in Figure 3d, for those atoms associated with monohydride). As a result of this charge distribution change, the polarity of the boundary B–N bond after fluorination increases, approaching that in the bulk. A similar boundary improvement and thus an improved charge distribution are also found for the hexagonal structures after fluorination, as indicated in Figure 3b when compared with Figure 3a. However, the extent of this change is considerably smaller than that of the cubic phase, as shown in Figure 3c,d. Thus, the extent of stabilization due to fluorination for the c-BN clusters is larger than that for the h-BN clusters. Consequently, both phases present their natural reactivities, with that over the hexagonal phase being considerably higher than that over the cubic phase, facilitating the desired etching selectivity.

To relate the etching mechanism of the H and F atoms over the h-BN and c-BN phases to the boundary saturation changes, we further examined the reactive sites of the H- and F-terminated clusters. In a small molecule, atoms with high reactivity can be

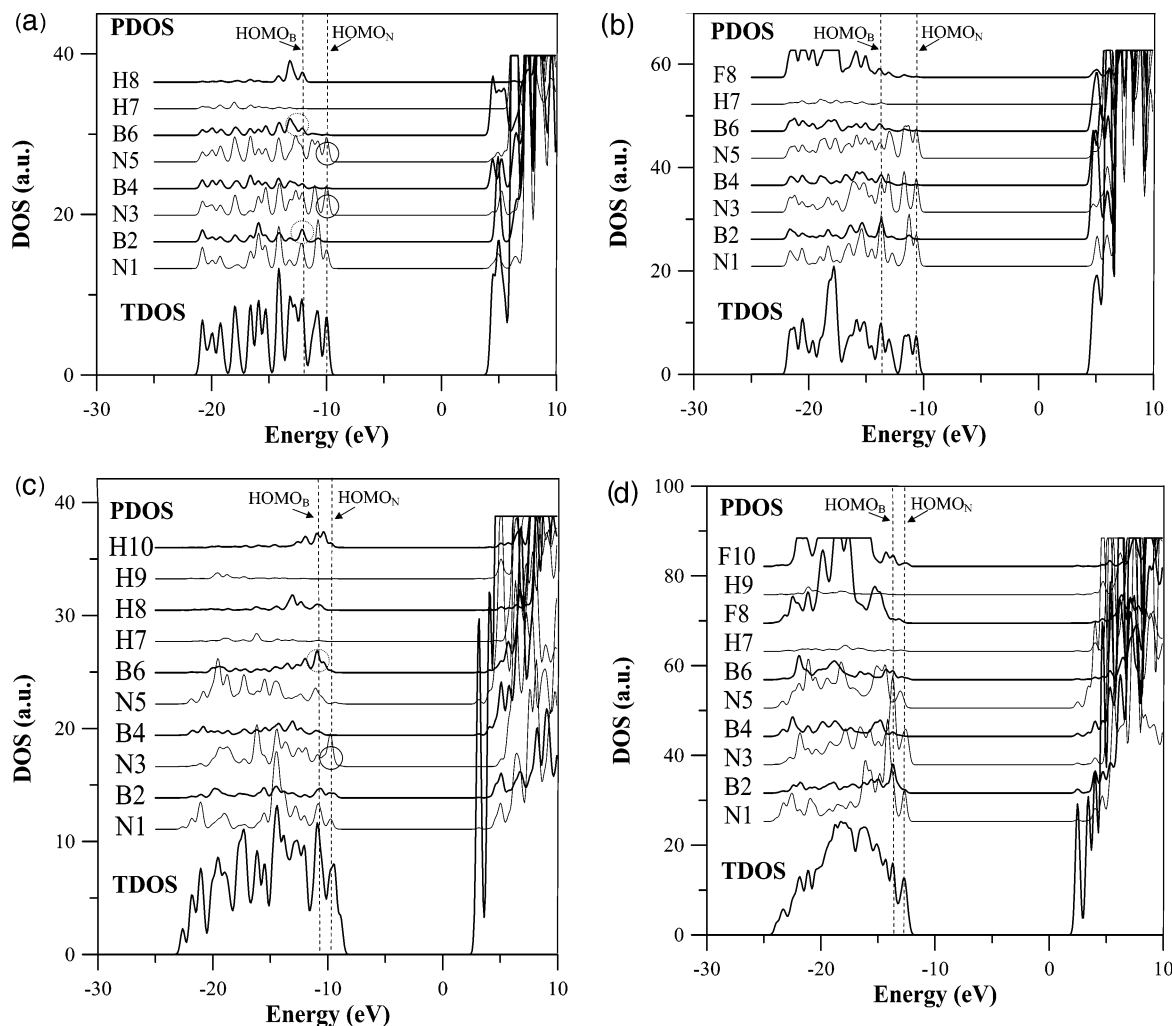


**Figure 4.** TDOS and PDOS of (a)  $\text{h-B}_{12}\text{N}_{12}(\text{H})$ , (b)  $\text{h-B}_{12}\text{N}_{12}(\text{F})$ , (c)  $\text{c-B}_{17}\text{N}_{17}(\text{H})$ , and (d)  $\text{c-B}_{17}\text{N}_{17}(\text{F})$  based on HF/6-31G\*\* calculations.

determined by checking the populations of atomic orbitals (AO) in the HOMO and LUMO. For large systems, as mentioned above, it would be more convenient to obtain such information by using the decomposition approach of DOS illustrated in our previous work.<sup>16</sup> By comparing the contribution of the partial DOS (PDOS) of the constituent atoms to the frontier orbitals, the reactive sites in a molecule can be determined. Figure 4 compares the total DOS (TDOS) and PDOS of four representative clusters (the same atomic labeling as in Figure 3 is used): the H-terminated  $\text{h-B}_{12}\text{N}_{12}(\text{H})$  and  $\text{c-B}_{17}\text{N}_{17}(\text{H})$  and the F-terminated  $\text{h-B}_{12}\text{N}_{12}(\text{F})$  and  $\text{c-B}_{17}\text{N}_{17}(\text{F})$ . For all four clusters, it can be seen clearly that the intensities of the PDOSs of the N atoms are considerably larger than those of the B atoms because the electrons in the latter are significantly stripped off. The HOMOs of the whole cluster are mainly located at the N atoms, while the HOMOs of boron atoms ( $\text{HOMO}_{\text{B}}$ ) lie inside their valence bands. The HOMOs of H or F atoms are generally located in the deep regions of the valence bands. However, in the case where only H atoms are used for the boundary saturation, the H atoms associated with the B atoms show many enhanced peaks in their PDOS and become closer to the top of the valence band (Figure 4a,c), indicating electron accumulation (consistent with the negative charges shown in Figure 3) and enhanced reactivity. As can be seen in Figure 4a,c, in cases of h-BN and c-BN with H atoms for boundary saturations, the HOMOs of the N atoms ( $\text{HOMO}_{\text{N}}$ ) are mainly located at the boundary N atoms, as indicated by solid circles (N3 and N5 for h-BN in Figure 4a; N3 for c-BN in Figure 4c), while

$\text{HOMO}_{\text{B}}$ s obviously receive more contribution from the boundary B atoms, as indicated by dashed circles (B2 and B6 for h-BN in Figure 4a; B6 for c-BN in Figure 4c). In contrast, upon fluorination (Figure 4b,d), these boundary atoms make contributions similar to those of bulk atoms or even smaller contributions, indicating the improper boundary conditions of the BN clusters terminated by hydrogen atoms have been improved and hence leading the clusters to a higher stability (or a lower reactivity) compared with the clusters before fluorination, especially for c-BN clusters. Moreover, the locations of HOMOs are generally shifted down upon fluorination with the c-BN showing the biggest effect, which is consistent with the largest reactivity decrease, as discussed earlier using frontier orbital theory. It should be noted that, even with fluorination, the reactivity of the boundary N atoms for h-BN clusters is still significant for h-BN, as shown by N3 in Figure 4b. It further provides the channel for the h-BN to be etched in addition to the overall high reactivity of this phase. A clear selective etching mechanism over the BN phases has thus been presented.

## Conclusion

Neither H nor F atoms selectively etch hydrogen-saturated h-BN. However, the etching selectivity during CVD growth of c-BN films would be effectively improved upon fluorination at the boron sites, which could be achieved by providing fluoride using  $\text{BF}_3$ . The fluorination results in a reasonable charge distribution among the atoms of the BN phases, in particular at

the boundary, leading to a significant decrease in the reactivity of the c-BN phase, thus increasing the etching selectivity. The enhanced etching selectivity would facilitate the synthesis of high-quality c-BN films via CVD for a wide range of advanced applications.

**Acknowledgment.** The work described in this paper is supported by a grant from the Research Grants Council of the Hong Kong Special Administrative Region, China [Project No. CityU 1011/01P].

## References and Notes

- (1) Mendes, R. C.; Corat, E. J.; Trava-Airoldi, V. J.; Ferreira, N. G.; Leite, N. F.; Iha, K. *Diamond Relat. Mater.* **1997**, *6*, 490.
- (2) Loh, K. P.; Foord, J. S.; Jackman, R. B.; Singh, N. K. *Diamond Relat. Mater.* **1996**, *5*, 231.
- (3) Zhang, R. Q.; Chu, T. S.; Lee, C. S.; Lee, S. T. *Chem. Vap. Deposition* **2000**, *6*, 227.
- (4) Zhang, R. Q.; Chu, T. S.; Lee, C. S.; Lee, S. T. *J. Phys. Chem. B* **2000**, *104*, 6761.
- (5) Kalss, W.; Haubner, R.; Lux, B. *Diamond Relat. Mater.* **1998**, *7*, 369.
- (6) Matsumoto, S.; Nishida, N.; Akashi, K.; Sugai, K. *J. Mater. Sci.* **1996**, *31*, 713.
- (7) Matsumoto, S.; Zhang, W. J. *Diamond Relat. Mater.* **2001**, *10*, 1868.
- (8) Zhang, W. J.; Matsumoto, S. *Chem. Phys. Lett.* **2000**, *330*, 243.
- (9) Zhang, W. J.; Matsumoto, S.; Kurashima, K.; Bando, Y. *Diamond Relat. Mater.* **2001**, *10*, 1881.
- (10) Larsson, K.; Carlsson, J. O. *J. Phys. Chem. B* **1999**, *103*, 6533.
- (11) Fukui, K.; Fujimoto, H. *Frontier Orbitals and Reaction Path: Selected Papers of Kenichi Fukui*; World Scientific: Singapore, 1997.
- (12) Hoffmann, R. *Rev. Mod. Phys.* **1988**, *60*, 601.
- (13) Zhang, R. Q.; Chu, T. S.; Cheung, H. F.; Wang, N.; Lee, S. T. *Phys. Rev. B* **2001**, *64*, 113304.
- (14) Zhang, R. Q.; Chan, K. S.; Zhu, R. S.; Han, K. L. *Phys. Rev. B* **2001**, *63*, 085419.
- (15) Zhang, R. Q.; Wang, J. J.; Dai, G. C.; Wu, J. A.; Zhang, J. P.; Xing, Y. R. *Chin. J. Semicond. (Overseas Ed.)* **1988**, *10*, 327.
- (16) Zhang, R. Q.; Lee, C. S.; Lee, S. T. *J. Chem. Phys.* **2000**, *112*, 8614.
- (17) Guerra, M. *Chem. Phys. Lett.* **1990**, *167*, 315.
- (18) Frisch, M. J.; Trucks, G. W.; Schlegel, H. B.; Scuseria, G. E.; Robb, M. A.; Cheeseman, J. R.; Zakrzewski, V. G.; Montgomery, J. A., Jr.; Stratmann, R. E.; Burant, J. C.; Dapprich, S.; Millam, J. M.; Daniels, A. D.; Kudin, K. N.; Strain, M. C.; Farkas, O.; Tomasi, J.; Barone, V.; Cossi, M.; Cammi, R.; Mennucci, B.; Pomelli, C.; Adamo, C.; Clifford, S.; Ochterski, J.; Petersson, G. A.; Ayala, P. Y.; Cui, Q.; Morokuma, K.; Malick, D. K.; Rabuck, A. D.; Raghavachari, K.; Foresman, J. B.; Cioslowski, J.; Ortiz, J. V.; Baboul, A. G.; Stefanov, B. B.; Liu, G.; Liashenko, A.; Piskorz, P.; Komaromi, I.; Gomperts, R.; Martin, R. L.; Fox, D. J.; Keith, T.; Al-Laham, M. A.; Peng, C. Y.; Nanayakkara, A.; Gonzalez, C.; Challacombe, M.; Gill, P. M. W.; Johnson, B.; Chen, W.; Wong, M. W.; Andres, J. L.; Gonzalez, C.; Head-Gordon, M.; Replogle, E. S.; Pople, J. A. *Gaussian 98*, Revision A.7; Gaussian, Inc.: Pittsburgh, PA, 1998.
- (19) Zhang, R. Q.; Chu, T. S.; Bello, I.; Lee, S. T. *Diamond Relat. Mater.* **2000**, *9*, 1774.
- (20) Zhang, R. Q.; Bertran, E.; Lee, S. T. *Diamond Relat. Mater.* **1998**, *7*, 1663.
- (21) Zhang, R. Q.; Chan, K. S.; Cheung, H. F.; Lee, S. T. *Appl. Phys. Lett.* **1999**, *75*, 2259.